Tailoring the Resonances of Nonlinear Mechanical Systems

T. Detroux, J.P. Noël, G. Kerschen

Space Structures and Systems Laboratory
Department of Aerospace and Mechanical Engineering
University of Liège, Belgium

Abstract

In this work we propose a novel optimization-based methodology to tailor nonlinear resonances of mechanical systems according to specific design objectives. The objective pursued herein is the realization of a predetermined frequency-amplitude or frequency-energy dependence of a structural mode. The proposed methodology consists in synthesizing the nonlinearities automatically, from low to large relative displacements, by optimizing piecewise-linear segments. The methodology is illustrated using 2-degree-of-freedom nonlinear systems with modal interaction suppression and isochronicity design applications.

Keywords: Modal design, nonlinear resonance, nonlinear normal mode, nonlinearity synthesis, restoring force.

Corresponding author:
Thibaut Detroux
Space Structures and Systems Laboratory
Department of Aerospace and Mechanical Engineering
University of Liège
Quartier Polytech 1, Allée de la Découverte 9 (B52/3)
B-4000 Liège, Belgium
Email: tdetroux@uliege.be

1 Introduction

The 20th century witnessed extraordinary advances in nonlinear systems theory. Today, engineers in academia and research centers are exploiting this theory to develop modeling, identification, simulation and control techniques. Even though important progress is yet to be achieved toward more effective and robust nonlinear methods, the next great challenge is to provide practitioners with methodologies to design with and for nonlinearity. This is the challenge the present paper attempts to address.

Since the 2000s, the benefits of nonlinearity have been more and more systematically explored in engineering. Among a variety of potential examples, the nonlinear implementation of signal processing operations is worthy of mention. In [1], tunable rectification was achieved using a granular crystal with bifurcating dynamics leading to quasiperiodic and chaotic states. By coupling nonlinear modes through internal resonances, Ref. [2] proposed a frequency stabilization mechanism for micromechanical resonators. In [3], a chain of nonlinear resonators involving a cascade of parametric resonances was also used to passively divide frequencies. Some further examples of advanced nonlinear design studies are to be found in the literature about wave propagation in smart materials. As an example, in [4], an array of spherical particles realized a nonlinear lens to transform an incident sound wave into a compact pulse of high acoustic energy, with applications in biomedical imaging and damage detection.

In the field of mechanical vibrations, intentionally utilizing nonlinearity has similarly gathered attention over the past few years. For instance, harvesting energy from ambient vibrations is a typical subject of research entailing nonlinear design [5]. Optimizing the nonlinear transient response by operating directly on the topology of the mechanical structure was also performed in [6]. Beyond the former examples, nonlinearity design in vibration engineering appears to attract most interest when it comes to shaping resonances.

Achieving design objectives through resonance tailoring has been used in the area of vibration absorption. The autoparametric absorber originally devised by Haxton and Barr is an example of this kind, where linear vibrations in a primary structure are passively attenuated by enforcing 2:1 resonance conditions with an attached beam-like absorber [7]. Oueini and co-workers developed to a large extent this early work by implementing quadratic feedback controllers and coupling them, in 2:1 autoparametric resonance, to the structural modes of linear multi-degree-of-freedom systems [8]. A related and substantial body of works concerns the mitigation of nonlinear vibrations as achieved, for example, by the nonlinear energy sink [9] or the nonlinear tuned vibration absorber [10]. For this latter absorber, the shaping of the two resonances of the coupled host structure-absorber system is based on the search for their equal magnitude as inspired by Den Hartog's linear design rule. Besides vibration absorption, a few other recent studies leveraged resonance tuning to meet design objectives that are less frequently addressed, like isochronicity [11], passive dynamical linearization [12] or extremely wide resonance patterns in microresonators [13]. Generally, a key step toward optimizing (in any sense) the behavior of a nonlinear resonance is the analysis of its parametric variability. Harmonic balance approaches are a standard tool for this purpose. Petrov applied such an algorithmic scheme to a large-scale

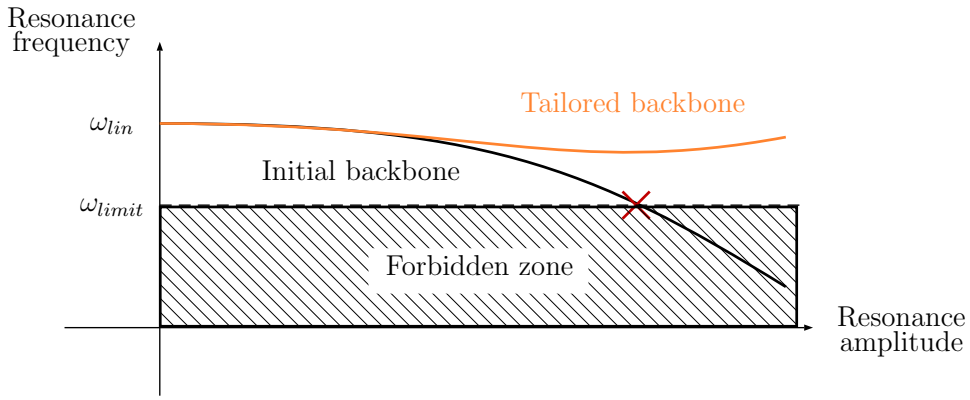

Figure 1: Schematic representation of resonance tailoring.

nonlinear bladed disk model involving complex contact interfaces [14]. Nonlinear antiresonances and bifurcations were characterized and tracked in a numerically similar way in Refs. [15] and [16], respectively. In the present paper, nonlinear resonance tailoring is performed by parametrizing nonlinear restoring forces using piecewise-linear functions and optimizing their coefficients using a harmonic balance technique.

The paper is organized as follows. Section 2 motivates the use of nonlinearity synthesis to tailor resonances of mechanical structures. The synthesis procedure and its implemetation are presented in Section 3, together with a numerical validation. In Section 4, the outlined methodology is applied to suppress modal interaction and to enforce isochronicity of nonlinear spring-mass systems. The conclusions of the study are finally drawn in the last section of the paper.

2 Problem statement for nonlinear resonance tailoring

In contrast to linear systems, the resonance frequencies of nonlinear systems depend on motion amplitude. For instance, a nonlinear system is said to be hardening (softening) when the resonance frequencies increase (decrease) for increasing amplitudes. The locus of resonance frequencies as a function of the amplitude is termed *backbone curve*.

Depending on the design problem at hand, the dynamicist might want to tailor the backbone curve such that the considered system features a desired resonance frequency at a specific amplitude. Figure 1 illustrates this idea for a nonlinear system featuring a softening nonlinearity. From a specific amplitude at resonance, the resonance frequency of interest enters into a zone forbidden by design, e.g., a zone where the system might resonate with surrounding structures. The backbone curve should thus be modified such that this problem is avoided. One possible way is to introduce an additional nonlinearity with restoring force $g(x)$ into the system, either at the location of the existing nonlinearity or at another location.

The tailoring of resonance frequencies through nonlinearity synthesis represents the main objective of this paper. As illustrated in Fig. 2, the sought backbone curve is discretized by target points $\left(\omega^*_{(k)}, A^*_{(k)}\right)$ with $k = 1, \ldots, n_t$. Similarly, the optimized restoring force $g(x)$ is discretized into $2n_t + 1$ intervals defined by points $l_{(k)}, \ldots, l_0, u_0, \ldots, u_{(k)}$. In this work, $g(x)$ is assumed to be odd and symmetric. It is also equal to zero in the (arbitrarily small) interval $[l_0, u_0]$ around the origin. Consequently, the optimization is to be carried out in n_t intervals $[u_0, u_1], \ldots, [u_{n_t-1}, u_{n_t}]$.

To calculate the backbone curve, the nonlinear normal mode (NNM) theory (see, e.g., [17]) is used. The undamped and unforced system is considered:

$$\mathbf{M}\ddot{\mathbf{q}} + \mathbf{K}\mathbf{q} + \mathbf{f}_{nl}(\mathbf{q}) = \mathbf{0} \tag{1}$$

where $\mathbf{M}$ and $\mathbf{K}$ are the mass and stiffness matrices, respectively, whereas $\mathbf{q}$ is the displacement vector. The vector $\mathbf{f}_{nl}(\mathbf{q}) = \tilde{\mathbf{f}}_{nl}(\mathbf{q}) + g(x)\mathbf{e}_i - g(x)\mathbf{e}_j$ comprises the restoring forces $\tilde{\mathbf{f}}_{nl}$ and $g(x)$ of the original and synthesized nonlinearities, respectively. $x = q_i - q_j$ is the relative displacement at the location of the additional nonlinearity, and $\mathbf{e}_i$ and $\mathbf{e}_j$ are vectors of zeros with a value of one at the degree of freedom (DOF) i and j, respectively.

3 Automatic nonlinearity synthesis procedure

3.1 The optimization algorithm

The proposed algorithm is presented in Fig. 3. To greatly facilitate the process, the restoring force $g(x)$ is optimized piece by piece. Doing so, the restoring force is approximated using piecewise-linear segments. The interval $[u_0, u_1]$ is first considered, and variable $g_{(1)}$ is optimized using classical Newton-Raphson iterations until the backbone curve comprises the target point $\left(\omega^*_{(1)}, A^*_{(1)}\right)$. When convergence is obtained, $g_{(1)}$ is frozen, and variable $g_{(2)}$ is optimized. The process stops when the interval $[u_{n_t-1}, u_{n_t}]$ has been considered, and the backbone curve passes through all target points.

Considering now the kth interval $[u_{k-1}, u_k]$, the optimization problem

$$\min_{\mathbf{z}_{(k)}, g_{(k)}} \left\| \begin{array}{c} \mathbf{h} \\ \Delta A \end{array} \right\| \tag{2}$$

is solved until the objective function is zero. As explained in the next section, $||\mathbf{h}|| = 0$ enforces a NNM motion of fundamental frequency $\omega^*_{(k)}$. $\Delta A = A_{(k)} - A^*_{(k)} = 0$ where $A_{(k)} = \max_t \left|q_{m(k)(t)}\right|$ ensures that the maximum amplitude of the NNM motion at the selected DOF q_m is equal to the target amplitude $A^*_{(k)}$.

The optimization variables $\mathbf{z}_{(k)}$ and $g_{(k)}$ correspond to the Fourier coefficients of the NNM motion and to the value of the restoring force at $u_{(k)} = \max_t \left|q_{i(k)} - q_{j(k)}\right|$, respectively.

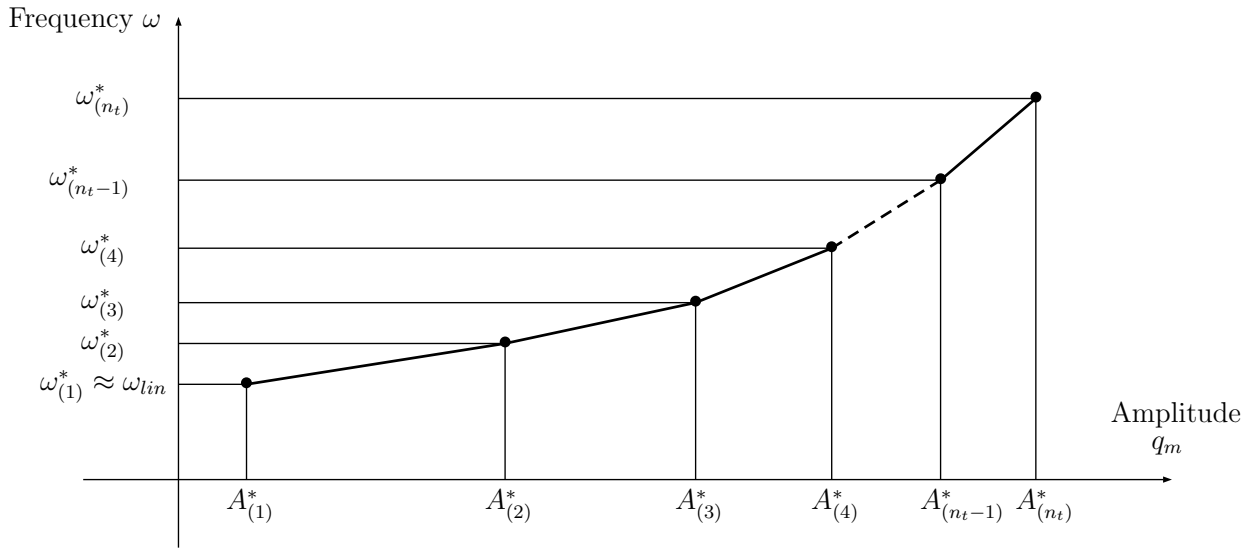

(a)

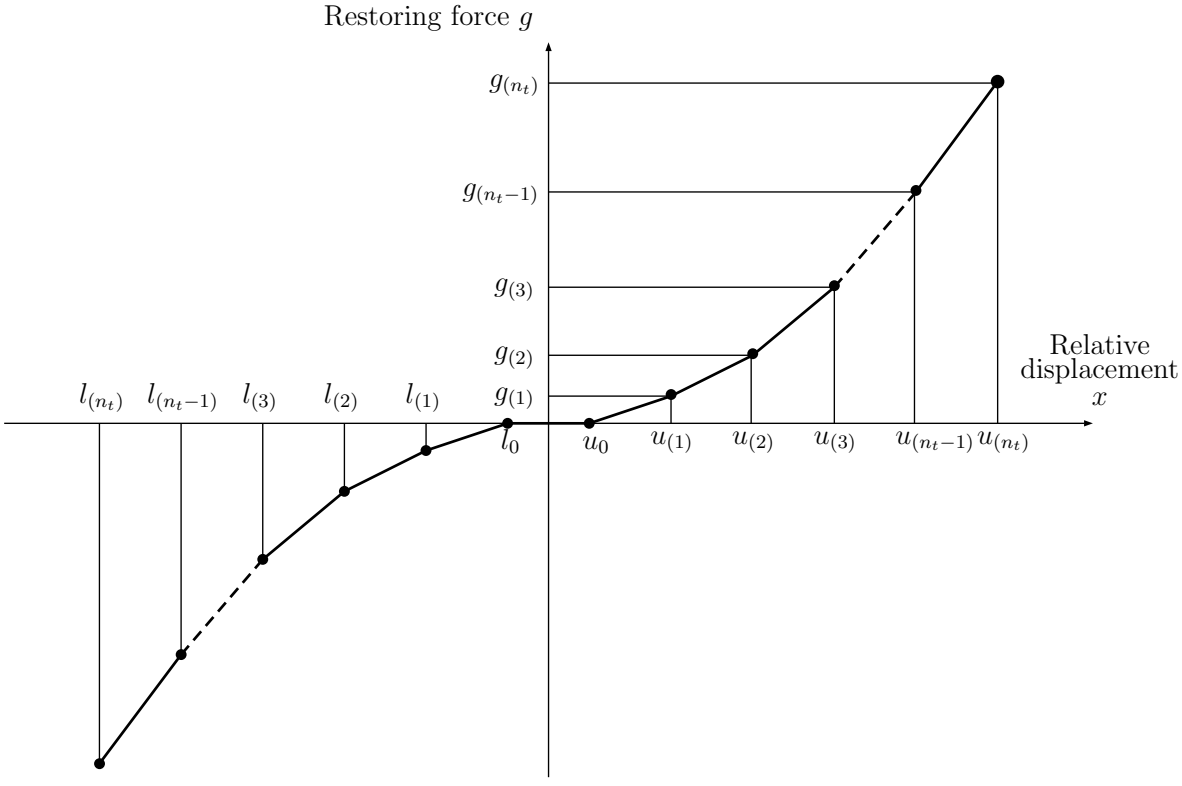

(b)

Figure 2: Sequential optimization procedure. (a) Frequency-amplitude plane with resonance target points; (b) synthesis of the restoring force $g(x)$.

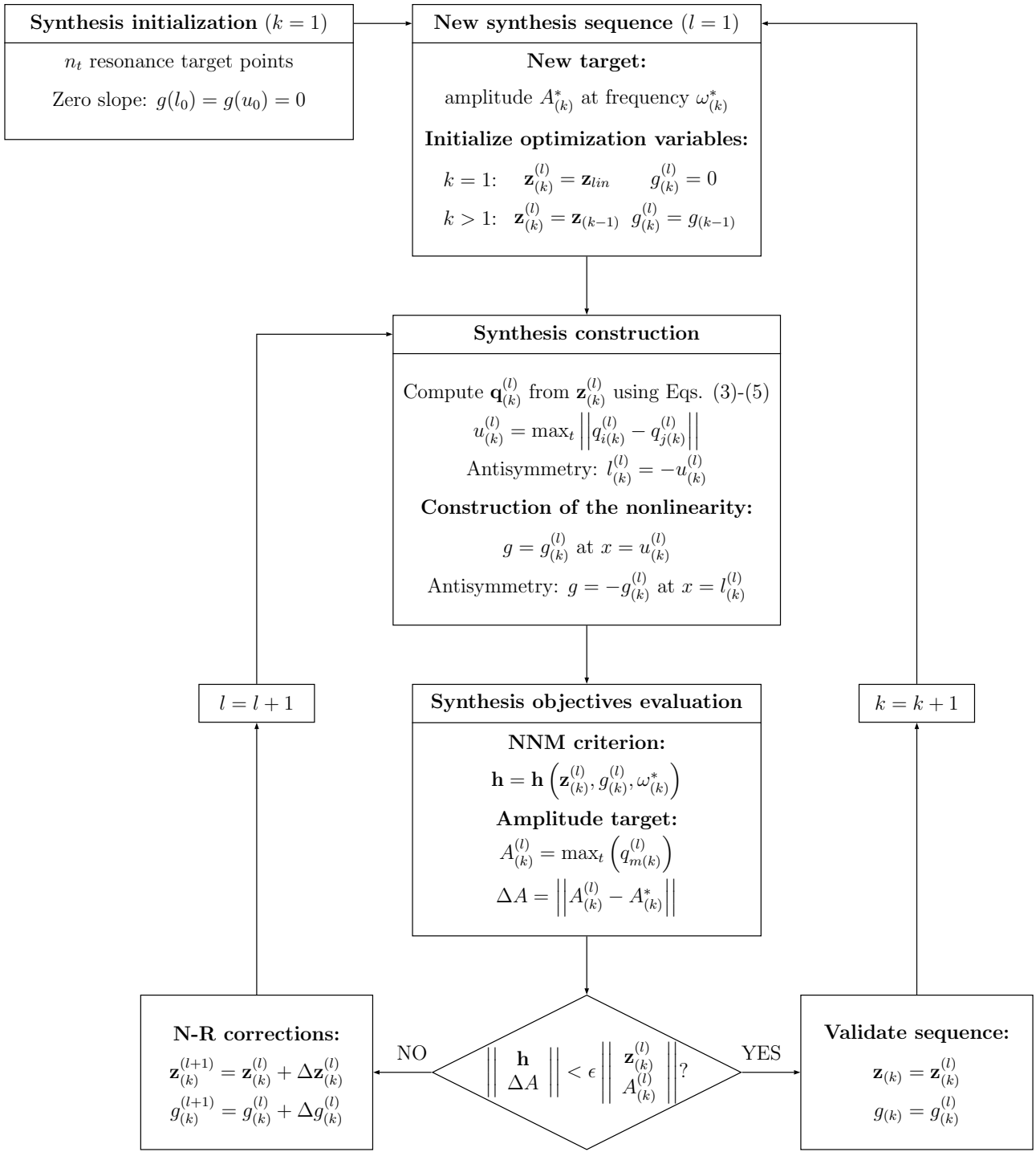

Figure 3: Algorithm for the nonlinearity synthesis procedure.

3.2 NNM calculation

The NNMs are calculated herein using a harmonic balance approximation with N_H harmonics:

$$\mathbf{q}(t) = \frac{\mathbf{c}_0^q}{\sqrt{2}} + \sum_{k=1}^{N_H} \left(\mathbf{s}_k^q \sin(k\omega t) + \mathbf{c}_k^q \cos(k\omega t)\right) \tag{3}$$

$$\mathbf{f}_{nl}(t) = \frac{\mathbf{c}_0^f}{\sqrt{2}} + \sum_{k=1}^{N_H} \left(\mathbf{s}_k^f \sin(k\omega t) + \mathbf{c}_k^f \cos(k\omega t)\right) \tag{4}$$

The Fourier coefficients of $\mathbf{f}_{nl}(t)$, $\mathbf{c}_k^f$ and $\mathbf{s}_k^f$, depend on the Fourier coefficients of the displacements $\mathbf{q}(t)$, $\mathbf{c}_k^q$ and $\mathbf{s}_k^q$, and on the restoring force $g(x)$. The Fourier coefficients are grouped into the $(2N_H+1)\,n \times 1$ vectors

$$\mathbf{z} = \left[\begin{array}{ccccccc} (\mathbf{c}_0^q)^{\mathrm{T}} & (\mathbf{s}_1^q)^{\mathrm{T}} & (\mathbf{c}_1^q)^{\mathrm{T}} & \dots & \left(\mathbf{s}_{N_H}^q\right)^{\mathrm{T}} & \left(\mathbf{c}_{N_H}^q\right)^{\mathrm{T}} \end{array}\right]^{\mathrm{T}} \tag{5}$$

$$\mathbf{b} = \left[\begin{array}{ccccccc} \left(\mathbf{c}_0^f\right)^{\mathrm{T}} & \left(\mathbf{s}_1^f\right)^{\mathrm{T}} & \left(\mathbf{c}_1^f\right)^{\mathrm{T}} & \dots & \left(\mathbf{s}_{N_H}^f\right)^{\mathrm{T}} & \left(\mathbf{c}_{N_H}^f\right)^{\mathrm{T}} \end{array}\right]^{\mathrm{T}} \tag{6}$$

where the operator $(\cdot)^{\mathrm{T}}$ denotes the transpose.

Substituting Eqs. (3-4) in Eq. (1) and balancing the harmonic terms with a Galerkin projection yields the equations of motion in the frequency domain [18]:

$$\mathbf{h}_{NNM}(\mathbf{z}, \omega, g) = \mathbf{A}(\omega)\mathbf{z} - \mathbf{b}(\mathbf{z}, g) = \mathbf{0} \tag{7}$$

where

$$\mathbf{A} = \left[\begin{array}{ccccccc} \mathbf{K} & & & & & & \\ & \mathbf{K}-\omega^2\mathbf{M} & & & & & \\ & & \mathbf{K}-\omega^2\mathbf{M} & & & & \\ & & & \ddots & & & \\ & & & & \mathbf{K}-(N_H\omega)^2\mathbf{M} & & \\ & & & & & \mathbf{K}-(N_H\omega)^2\mathbf{M} & \end{array}\right] \tag{8}$$

describes the linear dynamics.

A phase condition [19] is imposed by setting the Fourier coefficient of a DOF q_r to 0. This condition, in addition to Eq. (7), leads to the condition defining a NNM motion:

$$\mathbf{h} = \left[\begin{array}{c} \mathbf{h}_{NNM}(\mathbf{z}, \omega, g) \\ \mathbf{z}^{\mathrm{T}}\mathbf{e}_r \end{array}\right] = \mathbf{0} \tag{9}$$

Solving the nonlinear equations (9) involves several iterations on the Fourier coefficients $\mathbf{z}$ and on the restoring force $g(x)$. This is why condition (9) is added to the objective function (2).

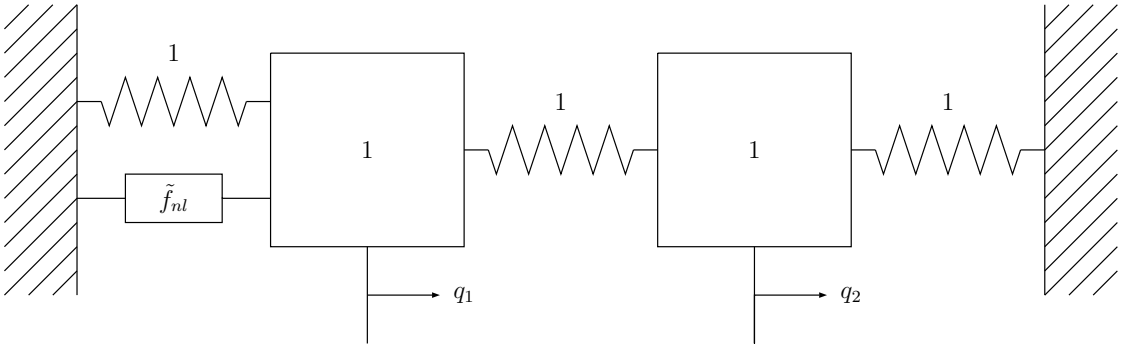

Figure 4: Schematic representation of the 2-DOF system (validation).

3.3 Validation of the synthesis methodology

The proposed methodology is demonstrated using the 2-DOF system sketched in Fig. 4, whose linear natural frequencies are $1\,\mathrm{rad/s}$ and $\sqrt{3}\,\mathrm{rad/s}$ for the in-phase and out-of-phase modes, respectively. A nonlinearity exists between the ground and the first DOF. The equations of motion of this system read:

$$\ddot{q}_1 + 2q_1 - q_2 + \tilde{f}_{nl}\left(x\right) = 0 \tag{10}$$

$$\ddot{q}_2 - q_1 + 2q_2 = 0 \tag{11}$$

Two different nonlinearities are considered, either a quintic nonlinearity $\tilde{f}_{nl1}$ or a piecewise-linear function $\tilde{f}_{nl2}$,

$$\tilde{f}_{nl1}\left(x\right) = x^5 \tag{12}$$

$$\tilde{f}_{nl2}\left(x\right) = \begin{cases} 2x+4 & (x<-2) \\ 0 & (-2\leq x\leq 2) \\ 2x-4 & (x>2) \end{cases} \tag{13}$$

The backbones of the first NNM computed by coupling the harmonic balance method with a continuation strategy [18] are represented in Fig. 5. A total of 9 harmonics ($N_H = 9$) are retained for all calculations presented in this paper. The black dots (ω^*, A^*) in Fig. 5 serve as target points for the synthesis algorithm.

Considering now the underlying linear system, a nonlinearity with an a priori arbitrary mathematical function $g(x)$ is introduced. The function $g(x)$ is optimized using the proposed algorithm until the corresponding backbone curve passes through all target points. The validation is successful if $g(x)$ is equal to the nonlinearity of the original system, i.e., either (12) or (13).

The nonlinear restoring forces synthesized by the optimizer are depicted in Fig. 6. An excellent agreement is observed between those and the original restoring forces, which demonstrates the effectiveness of our methodology.

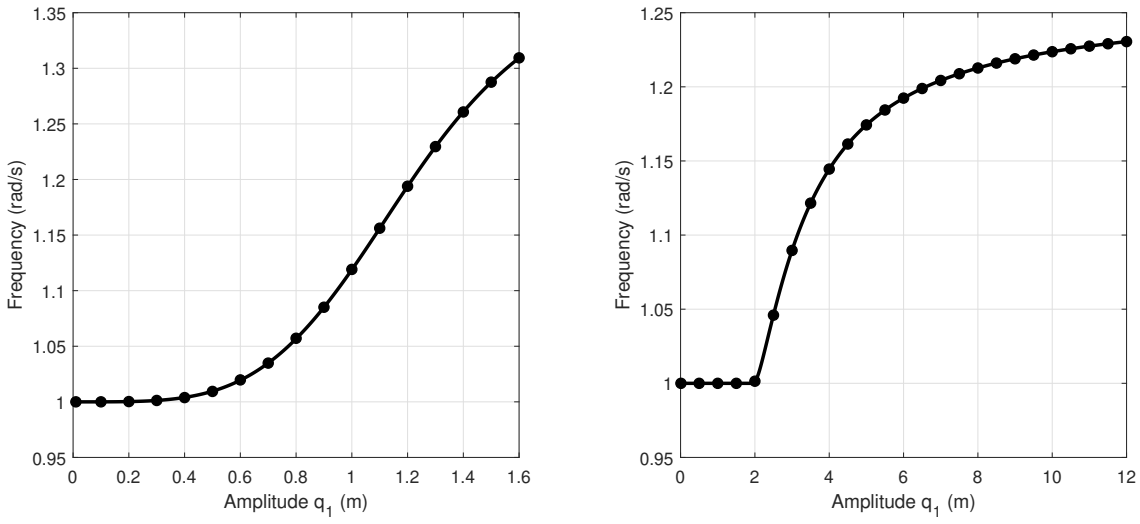

(a) (b)

Figure 5: Backbone of the first NNM: (a) quintic and (b) piecewise nonlinearity. The dots represents the selected target points.

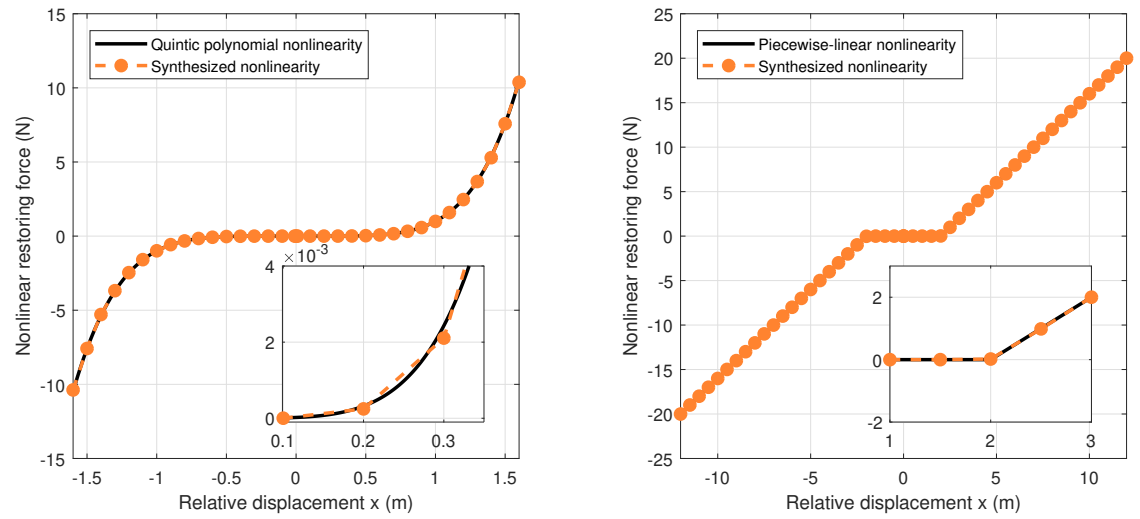

(a) (b)

Figure 6: Synthesized restoring force $g\left(x\right)$ for the (a) quintic polynomial and (b) piecewise-linear configurations (dashed lines) and comparison with the analytical expression (solid lines).

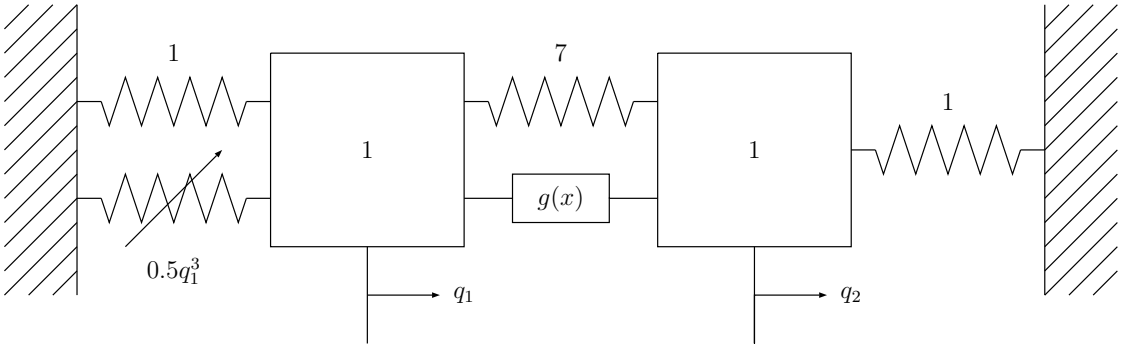

Figure 7: Schematic representation of the 2-DOF system (modal interaction suppression).

4 Application to modal interaction suppression and isochronicity

4.1 Modal interaction suppression

The 2-DOF system in Fig. 7 features a cubic nonlinerity between the ground and the first mass. The backbones of the first and second modes are depicted in Fig. 8(a). In this application, NNMs are represented in the frequency-energy plane, and target points are defined in terms of energy. The first backbone features an α-shaped loop near 1.3 rad/s. As explained in detail in [20], in that neighborhood, the frequency of the first mode is a third of the frequency of the second mode, which, in turn, triggers a 3:1 modal interaction between the two modes. The objective pursued in this section is to eliminate this modal interaction by translating the second NNM branch to lower energies, as shown schematically in Fig. 8(b). The 18 black dots (ω^*, E^*) serve as target points for the synthesis algorithm.

To this end, a nonlinearity $g\,(x)$ is introduced between the first and the second masses (*i.e.*, $x = q_1 - q_2$). The restoring force obtained after the synthesis procedure is represented in Fig. 9(a). The nonlinearity features a smooth hardening trend, which can be approximated by the high-order polynomial function

$$p(x) = 0.6257x^3 + 2.333x^5 - 0.4619x^7 + 0.03244x^9 \tag{14}$$

The resulting backbone for the first mode in Fig. 9(b) confirms that the modal interaction has been successfully eliminated.

4.2 Enforcing isochronicity

We now aim at enforcing isochronicity, *i.e.*, natural frequency invariance, for a specific vibration mode of a nonlinear system. The system in Fig. 10 exhibits a nonlinearity between the ground and the first mass. This softening-hardening polynomial nonlinearity is represented in Fig. 11(a) whereas the backbone of the first mode is depicted in Fig.

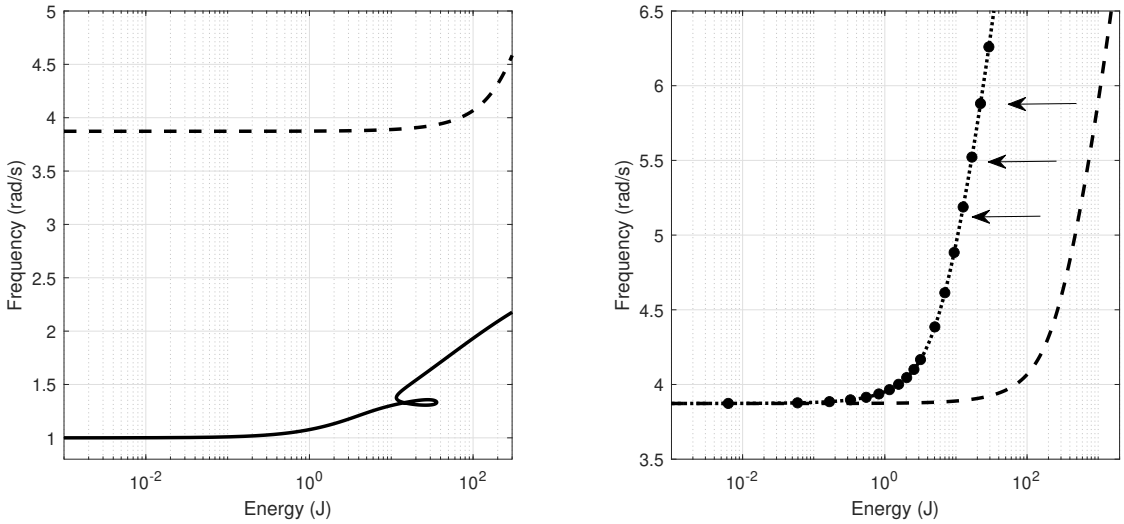

(a) (b)

Figure 8: Frequency-energy plot of the 2-DOF system (modal interaction suppression). (a) First (solid line) and second (dashed line) NNM branches of the primary system; (b) targeted second NNM branch for modal interaction suppression (dotted line) and associated target points (dots).

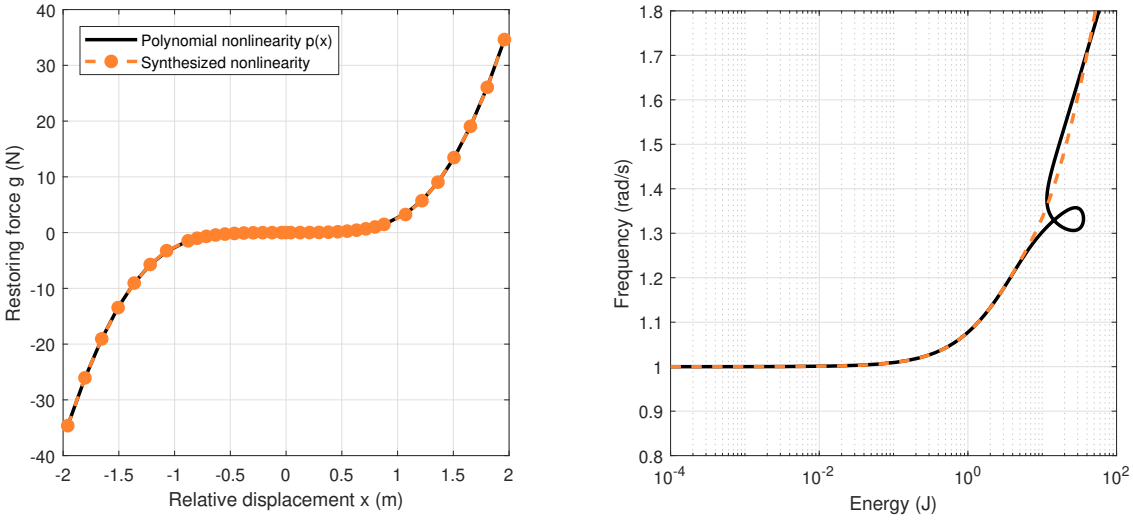

(a) (b)

Figure 9: Suppression of the 3:1 modal interaction. (a) Synthesized restoring force $g(x)$ (dashed line) and comparison with the fitted polynomial $p(x)$ (solid line); (b) backbone of the first NNM without (solid) and with (dashed) the synthesized nonlinearity.

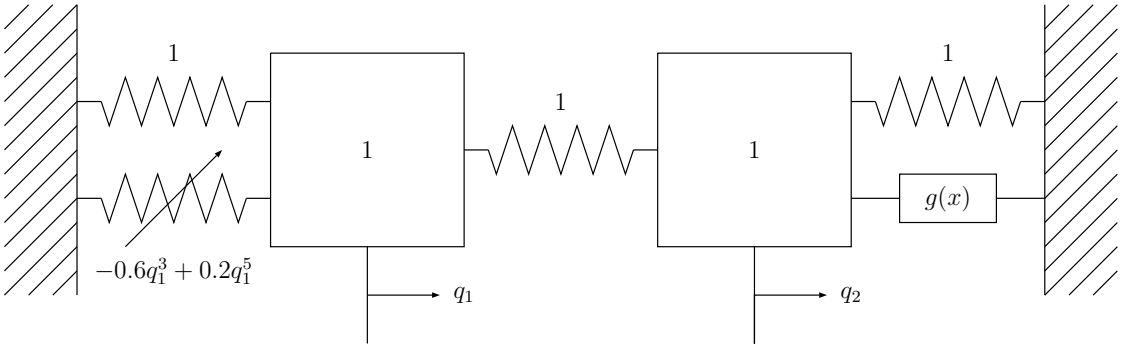

Figure 10: Schematic representation of the 2-DOF system (isochronicity).

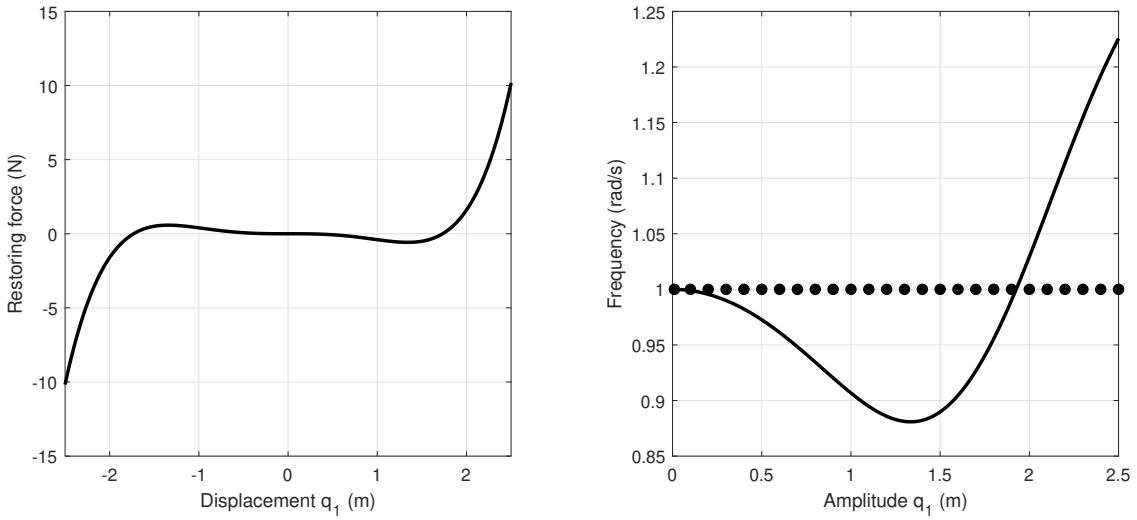

(a) (b)

Figure 11: Nonlinear features of the 2-DOF primary system. (a) Restoring force; (b) backbone of the first mode (line) and targets for isochronicity (dots).

11(b). The black dots (ω^*, A^*) aligned horizontally serve as target points to make the first natural frequency invariant.

An additional nonlinearity $g(x)$ is thus introduced between the ground and the second mass (*i.e.*, $x = q_2$). The calculated restoring force $g(x)$ is represented in Fig. 12. Interestingly, the synthesized nonlinearity features a smooth hardening-softening trend, which counterbalances the effect of the nonlinearity in the primary system.

In order to assess the performance of the optimized nonlinear system, we now study its damped, forced response under sine excitation:

$$\ddot{q}_1 + 0.1\dot{q}_1 - 0.05\dot{q}_2 + 2q_1 - q_2 - 0.6q_1^3 + 0.2q_1^5 = f\sin(\omega t) \tag{15}$$

$$\ddot{q}_2 - 0.05\dot{q}_1 + 0.1\dot{q}_2 - q_1 + 2q_2 + g(x) = 0 \tag{16}$$

Nonlinear frequency responses of the primary system with and without the synthesized nonlinearity are computed by combining harmonic balance and continuation [18]. Fig.

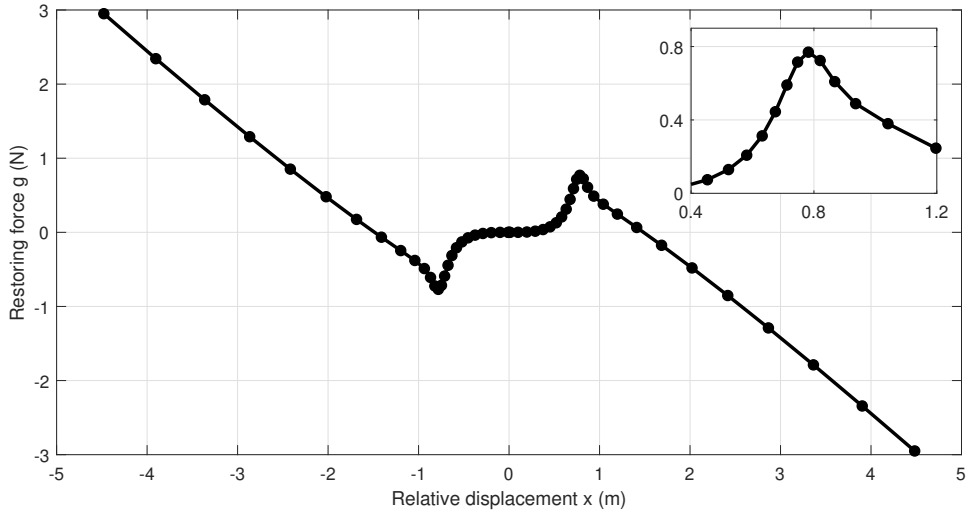

Figure 12: Synthesized restoring force $g\,(x)$ (isochronocity).

13 compares the responses obtained at different forcing levels. The first resonance of the primary system exhibits softening behavior up to 0.1 N, followed by hardening behavior. With the additional nonlinearity, the resonance frequency remains equal to 1 rad/s for the considered forcing levels, confirming that isochronocity for the first mode is achieved. Conversely, the second resonance peak does not seem to be affected by the additional nonlinearity.

The stability of the solutions of the optimized system for $f = 0.2\,\mathrm{N}$ and $0.5\,\mathrm{N}$ are shown in Fig. 14. In both cases, branch point bifurcations are detected on the left side of the resonance peak, resulting into stability changes and emanation of additional branches of periodic solutions. Interestingly, for $f = 0.5\,\mathrm{N}$, additional branch point and fold bifurcations generate another branch slightly shifting the resonance peak to 1.015 Hz and make the resonance peak unstable. This result indicates that besides the mere optimization of the backbone, stability and bifurcation would also play a key role when designing nonlinear systems. This will be investigated in future studies.

5 Conclusions

The objective of this study was the development of an automatic design procedure for nonlinearity synthesis. This procedure provides the designers the freedom to tailor the frequency-amplitude or frequency-energy dependence of a nonlinear system according to their specific targets. Instead of optimizing the whole nonlinear restoring force at once, a sequential methodology was proposed to synthesize the restoring force piece-by-piece from low to large relative displacements, through the resolution of optimization subproblems with a limited number of design variables. The methodology and the piecewise-linear modeling of the restoring force proved successful, even to capture nonlinearities with polynomial or nonsmooth behaviors. The nonlinearity synthesis was also demonstrated

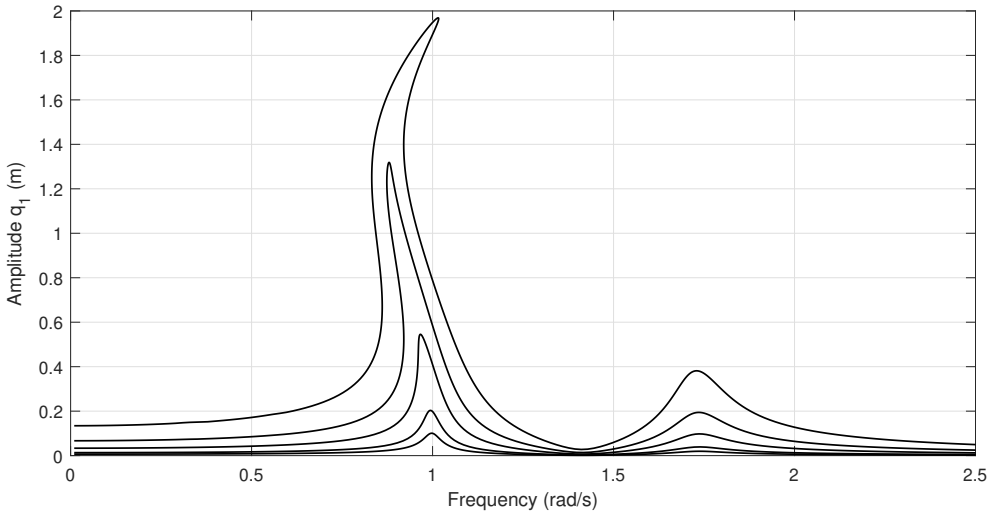

(a)

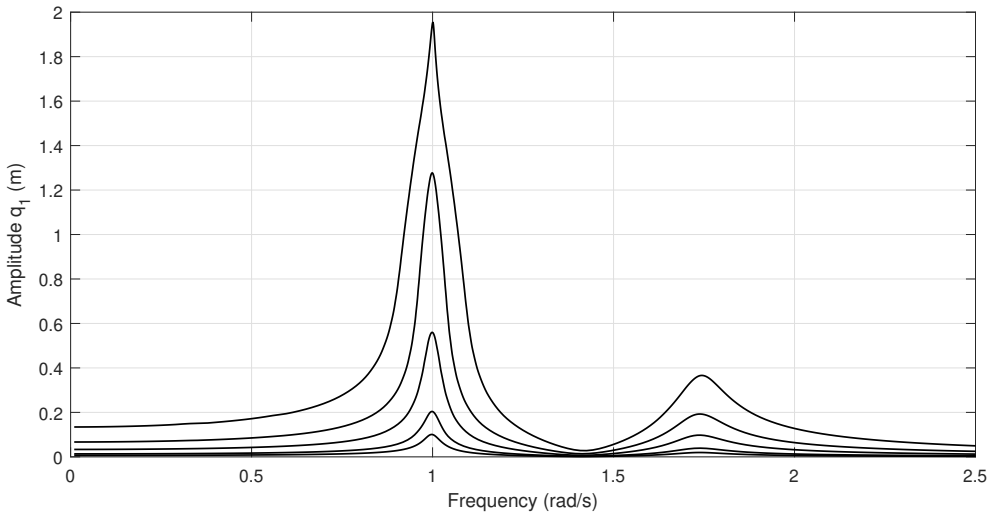

(b)

Figure 13: Nonlinear frequency responses for $f = 0.01\,\mathrm{N}$, $0.02\,\mathrm{N}$, $0.05\,\mathrm{N}$, $0.1\,\mathrm{N}$ and $0.2\,\mathrm{N}$. Without (a) and with (b) the synthesized nonlinearity.

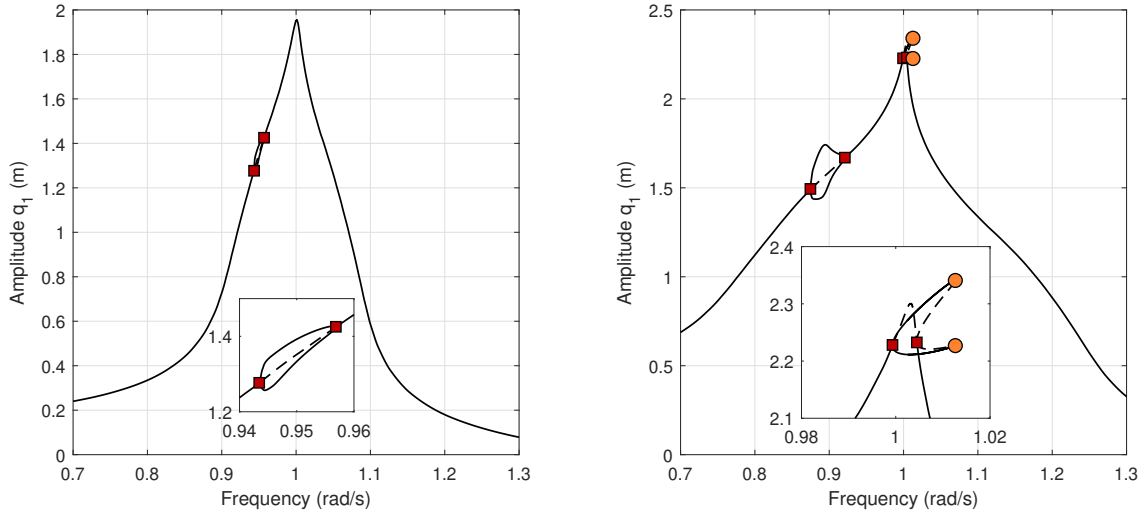

(a) (b)

Figure 14: Nonlinear frequency responses for (a) $f = 0.2\,\mathrm{N}$ and (b) $f = 0.5\,\mathrm{N}$. Stable and unstable solutions are represented with solid and dashed lines, respectively. Fold and branch point bifurcations are represented with circle and square markers, respectively.

useful to suppress modal interactions, and impose mode isochronicity.

The perspectives of this work include the extension of the procedure to address multi-modal objectives through the synthesis of multiple nonlinear connections. More flexible modeling of the connection will be studied, including piecewise-polynomial and non-symmetric functions to describe the restoring forces. It is also known that several nonlinear systems may feature frequency-amplitude or frequency-energy dependance; in this context, the unicity of the synthesized solutions will also be investigated.

Acknowledgments

The author T. Detroux is a Postdoctoral Researcher of the Fonds de la Recherche Scientifique - FNRS which is gratefully acknowledged. The authors J.P. Noël and G. Kerschen would like to acknowledge the financial support of the SPW (WALInnov grant).

References

[1] N. Boechler, G. Theocharis, C. Daraio, Bifurcation-based acoustic switching and rectification, *Nature Materials* 10, 665-668, 2011.

[2] D. Antonio, D.H. Zanette, D. Lopez, Frequency stabilization in nonlinear micromechanical oscillators, *Nature Communications* 3, 806, 2012.

[3] B.S. Strachan, S.W. Shaw, O. Kogan, Subharmonic resonance cascades in a class of coupled resonators, *Journal of Computation and Nonlinear Dynamics* 8(4), 041015, 2013.

[4] A. Spadoni, C. Daraio, Generation and control of sound bullets with a nonlinear acoustic lens, *Proceedings of the National Academy of Sciences* 107, 7230, 2010.

[5] A. Karami, D.J. Inman, Powering pacemakers from heartbeat vibrations using linear and nonlinear energy harvesting, *Applied Physics Letters* 100, 042901, 2012.

[6] S. Dou, B.S. Strachan, S.W. Shaw, J.S. Jensen, Structural optimization for nonlinear dynamic response, *Philosophical Transactions of the Royal Society A* 373, 20140408, 2015.

[7] R.S. Haxton, A.D.S. Barr, The autoparametric vibration absorber, *ASME Journal of Engineering for Industry* 94(1), 119-125, 1972.

[8] S.S. Oueini, A.H. Nayfeh, J.R. Pratt, A nonlinear vibration absorber for flexible structures, *Nonlinear Dynamics* 15, 259-282, 1998.

[9] A.F. Vakakis, O.V. Gendelman, L.A. Bergman, D.M. McFarland, G. Kerschen, Y.S. Lee, Nonlinear Targeted Energy Transfer in Mechanical and Structural Systems, Springer, 2009.

[10] G. Habib, T. Detroux, R. Viguié, G. Kerschen, Nonlinear generalization of the Den Hartog's equal-peak method, *Mechanical Systems and Signal Processing* 52-53, 17-28, 2015.

[11] I. Kovacic, R.H. Rand, About a class of nonlinear oscillators with amplitude-independent frequency, *Nonlinear Dynamics* 74, 455-465, 2013.

[12] G. Habib, C. Grappasonni, G. Kerschen, Passive linearization of nonlinear resonances, *Journal of Applied Physics* 120, 044901, 2016.

[13] R. Potekin, K. Asadi, S. Kim, L.A. Bergman, A.F. Vakakis, H. Cho, Ultrabroadband microresonators with geometrically nonlinear stiffness and dissipation, *Physical Review Applied* 13, 014011, 2020.

[14] E.P. Petrov, Direct parametric analysis of resonance regimes for nonlinear vibrations of bladed disks, *ASME Journal of Turbomachinery* 129(3), 495-502, 2007.

[15] A. Renault, O. Thomas, H. Mahé, Numerical antiresonance continuation of structural systems, *Mechanical Systems and Signal Processing* 116, 963-984, 2019.

[16] C. Grenat, S. Baguet, C.H. Larmarque, R. Dufour, A multi-parametric recursive continuation method for nonlinear dynamical systems, *Mechanical Systems and Signal Processing* 127, 276-289, 2019.

[17] G. Kerschen, M. Peeters, J.C. Golinval, A.F. Vakakis, Nonlinear normal modes, Part I: A useful framework for the structural dynamicist, *Mechanical Systems and Signal Processing* 23(1), 170-194, 2009.

[18] T. Detroux, L. Renson, L. Masset, G. Kerschen, The harmonic balance method for bifurcation analysis of large-scale nonlinear mechanical systems, *Computer Methods in Applied Mechanics and Engineering* 296, 18-38, 2015.

[19] R. Seydel. *Practical bifurcation and stability analysis*. Springer-Verlag, New-York, NY, 2010.

[20] M. Peeters, G. Kerschen, J.C. Golinval, Dynamic testing of nonlinear vibrating structures using nonlinear normal modes, *Journal of Sound and Vibration* 330(3),486-509, 2011.